HEALTH AND MEDICINE

Pregnancy and postpartum dynamics revealed by millions of lab tests

Alon Bar[1]†, Ron Moran[1]†, Netta Mendelsohn-Cohen[2], Yael Korem Kohanim[3], Avi Mayo[1], Yoel Toledano[4], Uri Alon[1]*

Pregnancy and delivery involve dynamic alterations in many physiological systems. However, the physiological dynamics during pregnancy and after delivery have not been systematically analyzed at high temporal resolution in a large human population. Here, we present the dynamics of 76 lab tests based on a cross-sectional analysis of 44 million measurements from over 300,000 pregnancies. We analyzed each test at weekly intervals from 20 weeks preconception to 80 weeks postpartum, providing detailed temporal profiles. About half of the tests take 3 months to a year to return to baseline postpartum, highlighting the physiological load of childbirth. The precision of the data revealed effects of preconception supplements, overshoots after delivery and intricate temporal responses to changes in blood volume and renal filtration rate. Pregnancy complications—gestational diabetes, preeclampsia, and postpartum hemorrhage—showed distinct dynamical changes. These results provide a comprehensive dynamic portrait of the systems physiology of pregnancy.

INTRODUCTION

During pregnancy, the mother undergoes physiological changes that support fetal growth and development. The cardiovascular, respiratory, renal, gastrointestinal, skeletal, metabolic, endocrine, and immune systems are all affected by fetal demand and massive endocrine secretion by the placenta (*1*–*4*). Elevated demand for oxygen and nutrients causes an increase in cardiac output and up to 50% growth in blood volume (*1*). The kidneys increase the glomerular filtration rate, leading to increased urine production (*1*). The immune system is modulated to prevent rejection of the fetus, and coagulation and red blood cells show marked changes (*1*, *2*, *5*). Metabolism shifts to increased insulin resistance and lipid production to supply energy for fetal growth (*6*).

Delivery marks a profound change as the fetus and placenta exit the body and abruptly cease their metabolic and endocrine effects. The mother undergoes a series of adaptations in which various physiological systems recover with different timescales—from hours to months (*7*). Pregnancy and postpartum periods have an increased risk of complications including gestational diabetes, postpartum hemorrhage (PPH), anemia, depression, and eclampsia (*8*).

Understanding healthy physiology and pathology is essential for both advancing basic science and as a baseline for treatment. This understanding of the physiological changes during pregnancy and postpartum requires precise temporal data on numerous physiological parameters. However, existing studies have a limited number of participants, consider only a few parameters, and have low temporal resolution, typically of one time point per trimester (*9*, *10*). Knowledge is even more sparse in the postpartum period in which a single time point is usually measured. Meta-analyses have collected these smaller studies to construct normal ranges for tests in each trimester (*9*, *10*). Together, our knowledge of the physiological time course is thus limited to low temporal resolution. Here, we harness a large national health record database (*11*) to study over 300K pregnancies in terms of 76 major lab tests, totaling over 43 million tests. We cross-sectionally analyzed these test results at weekly time intervals, and we present this information as a resource. We identify global dynamical trends in healthy pregnancies and in pregnancy complications.

RESULTS

We composed a dataset of lab tests throughout pregnancy and postpartum

We obtained data from Clalit Healthcare, the largest health maintenance organization (HMO) in Israel, with over 5 million members as of 2024, with broad socioeconomic and ethnic demographics (*11*, *12*). The HMO database includes about half of the pregnancies in Israel between 2003 and 2020. We analyzed 313,501 pregnancies of females aged 20 to 35 (Methods). The mean and median time of delivery was week 39 (Methods). This is an all-comers dataset, with stillbirths and multiple deliveries excluded. Demographic characteristics of the participants are presented in Table 1. We removed test values from individuals with disease codes or medications that statistically affect each test (Methods). Thus, we consider the dataset to include only healthy pregnancies.

In the period of 60 weeks before delivery to 80 weeks after delivery, we identified 44,312,918 test values from 110 lab tests (fig. S1 and table S1). We filtered out 34 tests due to high noise and/or low number of measurements (Methods) and retained 76 tests with a total of 43,498,258 measurements for analysis. Each test had between 36,043 and 1,652,191 measurement values. Our ethical agreement precluded longitudinal analysis of individual pregnancy trajectories. We therefore performed cross-sectional analysis—we aggregated each test over weekly intervals and analyzed them for summary statistics (Methods) including mean, median, and the (5, 10, 25, 50, 75, 90, and 95)th percentiles. For clarity, we highlight one test, alkaline phosphatase (ALP), in Fig. 1B and show all 76 profiles in Fig. 1C. Tests arranged by physiological systems are discussed in detail in Supplementary Text and fig. S2.

[1]Department of Molecular Cell Biology, Weizmann Institute of Science, Rehovot 7610001, Israel. [2]Department of Computer Science and Applied Mathematics, Weizmann Institute of Science, Rehovot 7610001, Israel. [3]Department of Immunobiology, Yale University School of Medicine, New Haven, CT, USA. [4]Division of Maternal Fetal Medicine, Helen Schneider Women's Hospital, Rabin Medical Center, Petah Tikva 4941492, Israel.
*Corresponding author. Email: urialonw@gmail.com
†These authors contributed equally to this work.

Table 1. Age and BMI of the study population. Because of privacy concerns, other demographics were not available. Age statistics are for all participants who had any of the 76 tests analyzed in the indicated week. Because of the cross-sectional nature of the dataset, each test and weekly interval is drawn from a different subcohort of the study population. IQR, interquartile range.

	60 weeks before delivery	At delivery	80 weeks postpartum
Age (mean, IQR)	28.2 (25.2–31.3)	28.3 (25.3–31.4)	29.3 (26.6–32.3)
BMI (mean, IQR)	24.6 (20.7–27.1)	28.8 (25.1–31.7)	26.0 (20.9–29.4)

Dynamic variation in pregnancy scales with homeostatic variation

All 76 mean test values varied across pregnancy and postpartum with a dynamic range of a few percent to hundreds of percent for different tests. The dynamic range of each test rises with its variation within the reference population—tests that vary widely between individuals also show large dynamic ranges during pregnancy and postpartum (Fig. 2A; Pearson correlation coefficient = 0.72, $P < 10^{-5}$) (Methods) with a linear relation. Thus, homeostatic processes seem to remain mostly within their physiological range. In the following analysis, we therefore use quantiles scores relative to a nonpregnant population. Quantile scores varied by 9 to 60 percentile points compared to reference, with a mean of 36 percentiles (Fig. 2B).

Dynamics show overshoots and undershoots after delivery

To understand the observed dynamics, we clustered tests according to their temporal profiles (Methods; Fig. 2, C to F, and fig. S4). We found four clusters, which define four profiles. Profile 1 rises during pregnancy and drops postpartum, and profile 2 is its mirror image, declining in pregnancy and rising postpartum. Profiles 3 and 4 show overshoots or undershoots at delivery followed by a return to preconception levels.

To understand the origin of the overshoots, we consider canonical physiological mechanisms (Supplementary Text). Pregnancy exerts a load on physiological variables to meet the needs of the mother and developing fetus. This load pushes physiological variables away from their normal set points or adjusts new set points that reflect physiological priorities (*13*, *14*). Upon delivery, this load is suddenly relaxed (Fig. 2L).

Variables without overshoot can be explained by first-order recovery to baseline [Fig. 2K(a)]. Variables are pushed by the load away from steady state during pregnancy and recover postpartum with a characteristic timescale, which follows the relaxation of the gestational load [Fig. 2, K(a) and M]. In this scenario, no overshoot occurs.

In contrast, an overshoot can occur when there exists an additional, slowly varying compensation mechanism [Fig. 2, K(b) and N], modeled here by an incoherent feed forward loop circuit (*15*, *16*). During pregnancy, the compensatory mechanism intensifies to keep the variable from moving too far from its set point. Upon delivery, the load is suddenly reduced but the compensation mechanism is still strong, causing overcompensation that induces an overshoot. Return to baseline of the variable is governed by the return of the compensation mechanism. An example is the slow growth of the thyroid gland during pregnancy that compensates for changes in the demand for thyroid hormones (*17*).

Other models can also provide the observed temporal shapes. For example, a load that grows during pregnancy and reduces during postpartum can provide alternative explanations for profiles 1 and 2. Delivery itself can serve as another source for rebound dynamics by forcing a sharp pulse in the opposite direction.

Physiological changes show slow postpartum recovery

To study the global temporal trajectories, we reduced dimensionality using principal components analysis (PCA) on the 76 tests at all 140-week intervals. The first two principal components capture 88% of the variation. The trajectory shows hysteresis—tests change during pregnancy and return to baseline via a different trajectory postpartum, as can be read by moving clockwise from conception in Fig. 3A.

Postpartum adaptation has two main phases, which are apparent on PC1 (Fig. 3A). Most changes take place in the 10 weeks after delivery, followed by a prolonged return to steady state. Many tests take months to return to baseline after delivery. To quantify the time to return to baseline, we use a measure from control theory called "settling time." The settling time is defined by the time after which the test remains within a small margin (here 0.2 SDs) of its postpartum baseline (Methods and Fig. 3B).

Approximately 41% (31/76) of the tests have long settling times that exceed 10 weeks (Fig. 3C). Among these are liver functions aspartate transaminase (AST) and alanine transaminase (ALT) that take about half a year to recover, metabolic factors such as cholesterol, and ALP, which settles only after about a year (Fig. 3C). Approximately 47% (36/76) of the tests settle rapidly within the first month. This includes all coagulation tests (Fig. 3C). The remaining ~12% of the tests (9/76) settle between 1 month and 10 weeks after delivery (Fig. 3C).

Slow return to baseline can arise from several factors. Metabolism is affected by the body mass index (BMI) that settles over months (*18*). Breastfeeding may also affect some tests, such as ALP, calcium, phosphate, parathyroid hormone (PTH), and prolactin (*19*). The dataset does not include information on who breastfed. About 90% of Israeli neonates are breastfed for a mean duration of about 70 days, and the rate of exclusive breastfeeding drops to about 60% at 2 months and to 20% at 6 months after birth (*20*).

Notably, several tests do not return to their preconception baseline after settling, including elevated levels of the inflammation marker complement-reactive protein (CRP), reduced thyroid-stimulating hormone (TSH), and reduced mean cell hemoglobin (MCH) and iron.

Preconception dynamics reflect health behaviors

We noticed that about a third of the tests (24/76) show dynamical trends before conception, in the period of 60 to 38 weeks before delivery (Fig. 4, A to C) (Methods). One of the strongest changes is a rise in folic acid (Fig. 4A). Folic acid supplements are taken in the

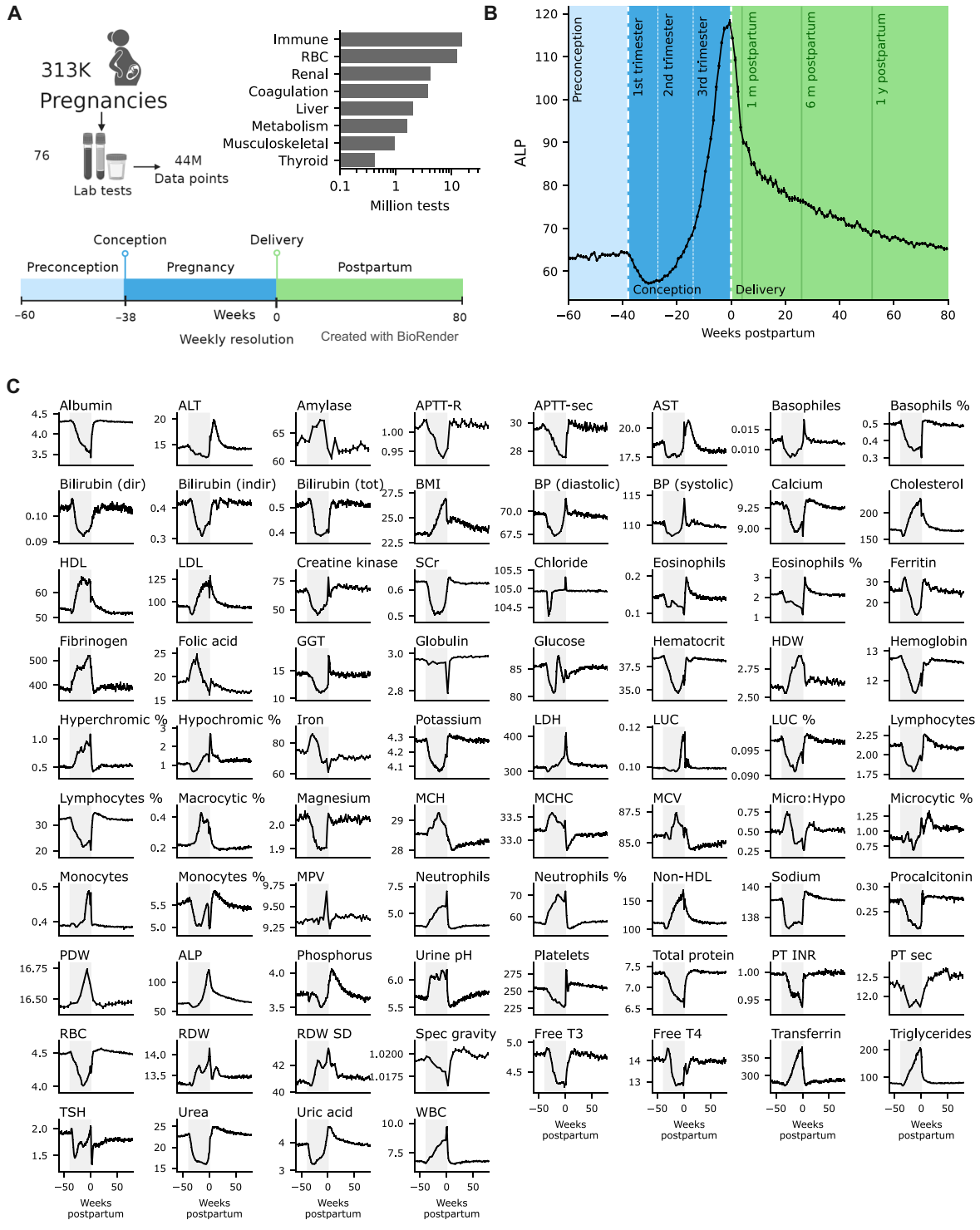

Fig. 1. Dataset of lab tests over preconception, pregnancy, and postpartum. (**A**) Schematic overview of the dataset. (**B**) Alkaline phsophatase (ALP) test (mean of the quantile-transformed values; see Methods) over 140 weeks. Error bars are SEM. Units are the standard for the test (IU/liter). m, months; y, year. (**C**) Seventy-six test values over 140 weeks; the period of pregnancy is in gray. For units and full test names, see table S1. Created with BioRender.

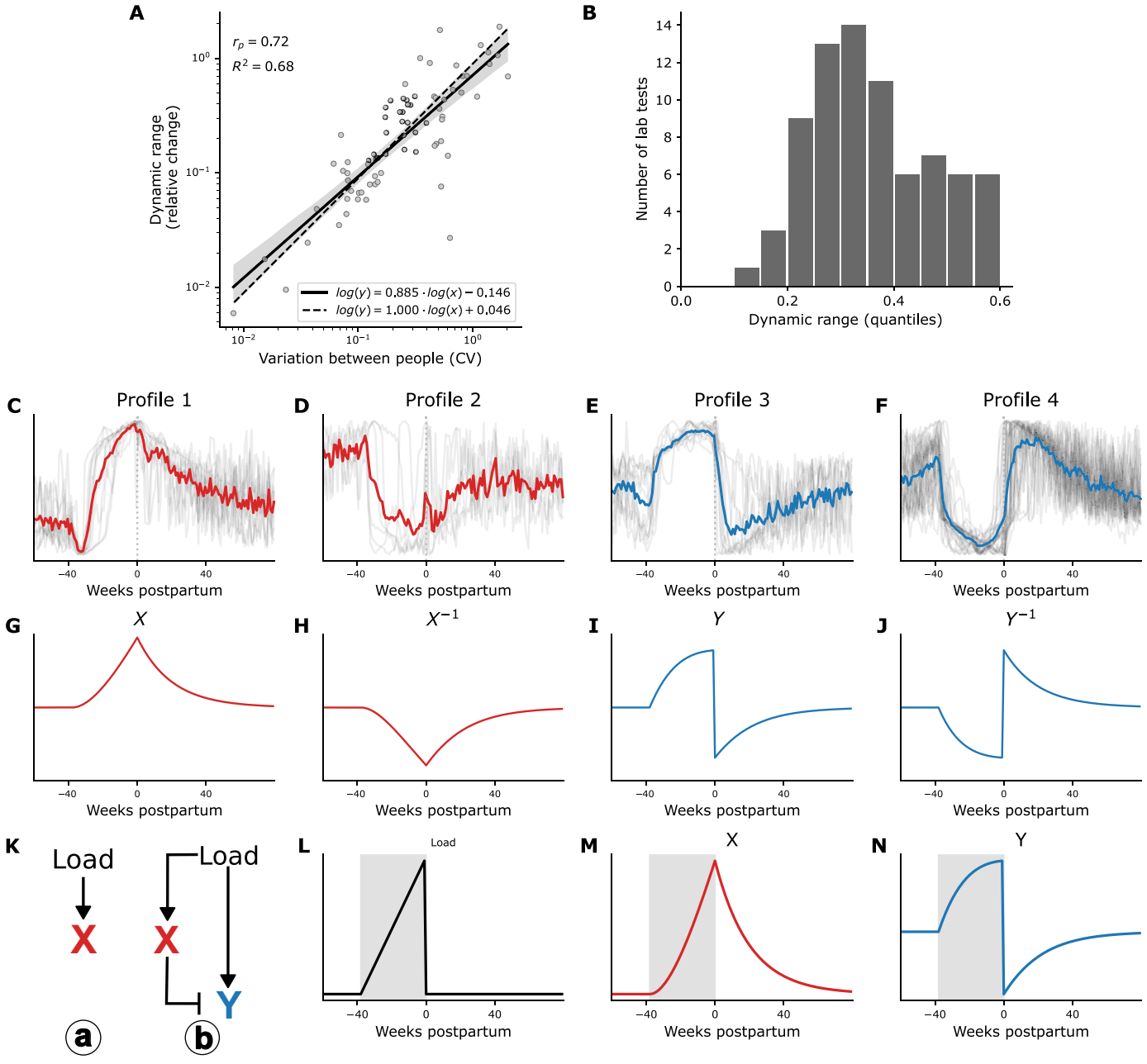

Fig. 2. Lab test dynamics vary during pregnancy and postpartum and can show overshoots and undershoots. (**A**) Relative dynamic range across the study period (Methods). Dynamic range (max-min)/(preconception average) is roughly proportional to the coefficient of variation (CV) of the test value in the reference population. r_p is the Pearson correlation. The dashed line within the 95% confidence interval has slope 1, $R^2 = 0.68$. (**B**) Histogram of the dynamic range of quantile scores of the 76 tests. (**C** to **F**) Four clusters of ranked test dynamical profiles. In gray are ranked individual tests; colored lines are cluster means. (**G** and **H**) Theoretical profiles for first-order response. (**I** and **J**) Theoretical profiles for a system with a slow compensatory mechanism. (**K**) Physiological circuits governing response to load and recovery. Full model found in Supplementary Text. (a) Circuit in which the load of pregnancy affects test X as a first-order system. (b) Circuit in which the load affects test Y with X as a compensatory system. (**L**) Pregnancy load in the theoretical model rises in pregnancy and drops abruptly at delivery. (**M**) First-order system X responds with no undershoot. (**N**) Compensated system Y shows an undershoot and a rebound effect.

months before conception by about half of the relevant population (*21*, *22*).

Supplements such as folic acid and vitamin B12 can exert physiological effects on other test values. These changes include a reduction in CRP (Fig. 4C), an increase in albumin (Fig. 4D), positive effects on anemia, anticoagulative effects, and lowering of lipids (*23*–*27*).

Some of the changes seen in preconception are not easily attributed to known effects of supplements. This includes changes in immune cell counts, ALT, AST, Na, urea, and urine pH. One possibility is that these tests are affected by yet unknown mechanisms by supplements or that they are affected by other preconception health behaviors such as reduced rates of smoking, alcohol consumption, and improved diet (*28*).

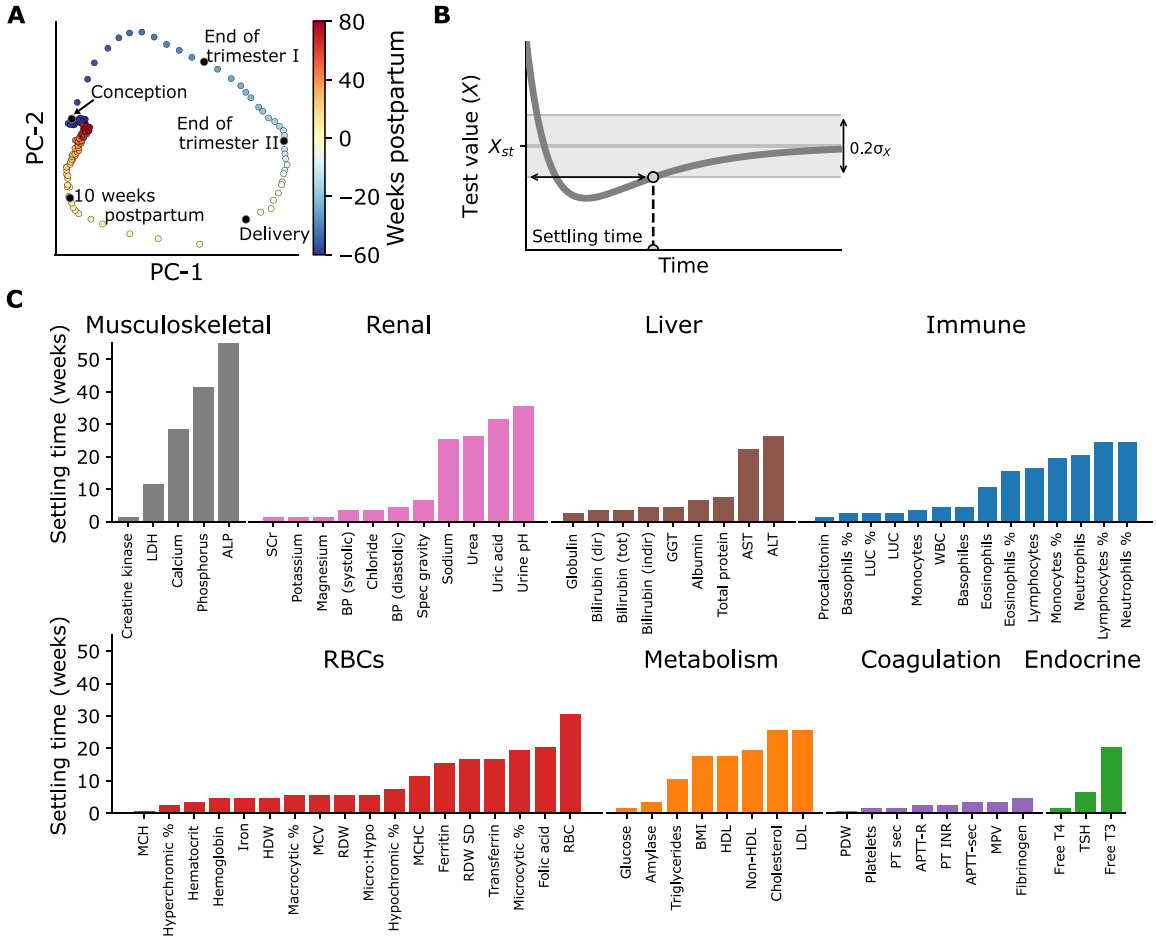

Fig. 3. Postpartum recovery times of tests range between days and a year. (**A**) Dimensionality reduction of test mean values as a function of time using PCA shows that the trajectory during pregnancy (blues) differs from the postpartum trajectory (orange and red). Each point is a week interval, progression clockwise from 60 weeks before delivery, through conception and delivery, to the end point 80 weeks after delivery. (**B**) Settling time is defined as the time after which the test remains within 0.2 SDs of its baseline. (**C**) Settling time of the tests in the dataset.

We conclude that the resolution and precision of the present dataset allows the detection of preconception changes that may correlate with health behaviors.

Complications of pregnancy show distinct dynamical changes

Thus far, we considered healthy pregnancies. To study complications of pregnancy, we analyzed data from pregnancies diagnosed with three major complications: preeclampsia (5629 pregnancies, 1.8%), gestational diabetes (7233 pregnancies, 2.3%), and PPH (4566 pregnancies, 1.5%). The incidence of these complications in the dataset is lower than expected (*29*–*31*). The lower incidence can be attributed to exclusion of risk factors, such as chronic illness (Methods) and maternal age over 35 years (*30*, *32*, *33*). We compared the test dynamics to healthy pregnancies during preconception, gestation, and postpartum (Fig. 5).

Preeclampsia is a complex disorder of pregnancy characterized by high blood pressure, headaches, and visual disturbances (*34*). In some cases [<2% of preeclamptic patients (*35*)], preeclampsia develops into eclampsia, a life-threatening condition usually requiring urgent delivery (*36*).

The causes of preeclampsia are not fully understood; it is believed to involve factors related to the placenta, the immune system, and genetics (*32*, *37*). We find that seven tests deviated significantly from the healthy reference (Fig. 6, A, D, G, and J). These include elevated platelets and ALT in the preconception period, elevated gestational uric acid, elevated postpartum triglycerides, and high systolic and diastolic blood pressure throughout the study period. High blood pressure during pregnancy is the main diagnostic tool for preeclampsia coupled with diagnosis of proteinuria (*37*).

PPH is a major cause of maternal morbidity and mortality characterized by excessive bleeding (≥1000 ml) after childbirth, typically within 24 hours after delivery and up to 12 weeks postpartum (*38*–*40*). The primary cause is uterine atony, where the uterus fails to contract adequately after delivery (*40*). Other causes include retained placental fragments, tears in the cervix or vaginal tissues, and coagulation disorders (*40*). We find that nine tests deviate significantly from the healthy reference, including tests before delivery (Fig. 6, B, E, H, and K). Platelets are mildly reduced, suggesting altered blood clotting even before pregnancy. Other coagulation markers are not significantly altered (*41*, *42*). PPH is also associated with a distinctive

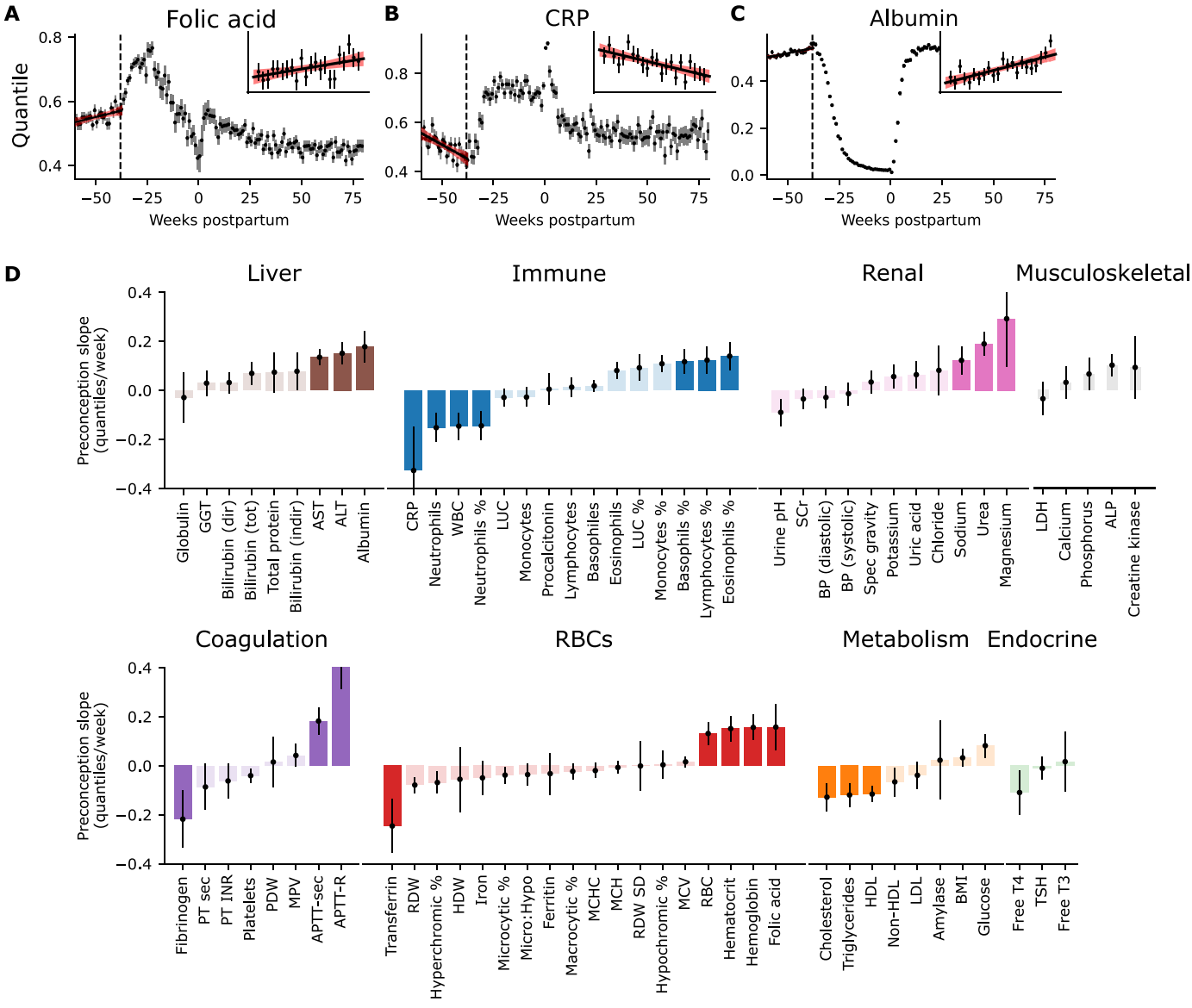

Fig. 4. Tests affected by health behaviors show preconception dynamics. (**A** to **C**) Folic acid, CRP, and albumin are examples of a strong preconception change. Mean conception time is indicated by a dashed line. The inset highlights the preconception period, red is regression with 95% confidence intervals. (**D**) Temporal slope of test values during preconception from linear regression. Tests are arranged by physiological system; tests in bold color have significant nonzero slope (>0.11 in absolute value and $P < 0.05$ adjusted for multiple comparisons, Benjamini-Hochberg). Error bars are 95% confidence intervals of slope.

pattern of decreased MCHC (mean corpuscular hemoglobin concentration) and elevated MCV (mean corpuscular volume) before conception and during gestation (Fig. 6K). This agrees with a longitudinal study where a higher MCV and MCH toward the end of pregnancy were associated with higher likelihood of PPH (*43*).

Gestational diabetes is characterized by high blood glucose that develops during pregnancy in females who did not previously have diabetes (*44*). It usually appears in the second or third trimester and can affect the health of both mother and fetus (*45*, *46*). We find that 20 tests deviate significantly from the healthy reference (Fig. 6, C, F, I, and L). This includes high glucose and HbA1c, elevated GGT liver damage test, and elevated triglycerides before and after pregnancy. These values are associated with obesity and inflammation, both causes of insulin resistance that contributes to gestational diabetes.

In all three complications, some of the significant changes are seen before conception or after delivery rather than during gestation (Fig. 6, J to L). In gestational diabetes, 17 of the 20 significantly different tests are different during preconception, of these 12 are statistically different solely in the preconception period. In other words, during gestation, the dynamical profiles are generally similar to healthy pregnancies. This is interesting given that tests for diagnosing pathologies such as gestational diabetes and preeclampsia are done during gestation (*47*, *48*).

DISCUSSION

We present a cross-sectional dataset of 40 million lab test measurements from 300,000 pregnancies during a 140-week period spanning preconception, gestation, and postpartum. The dataset is

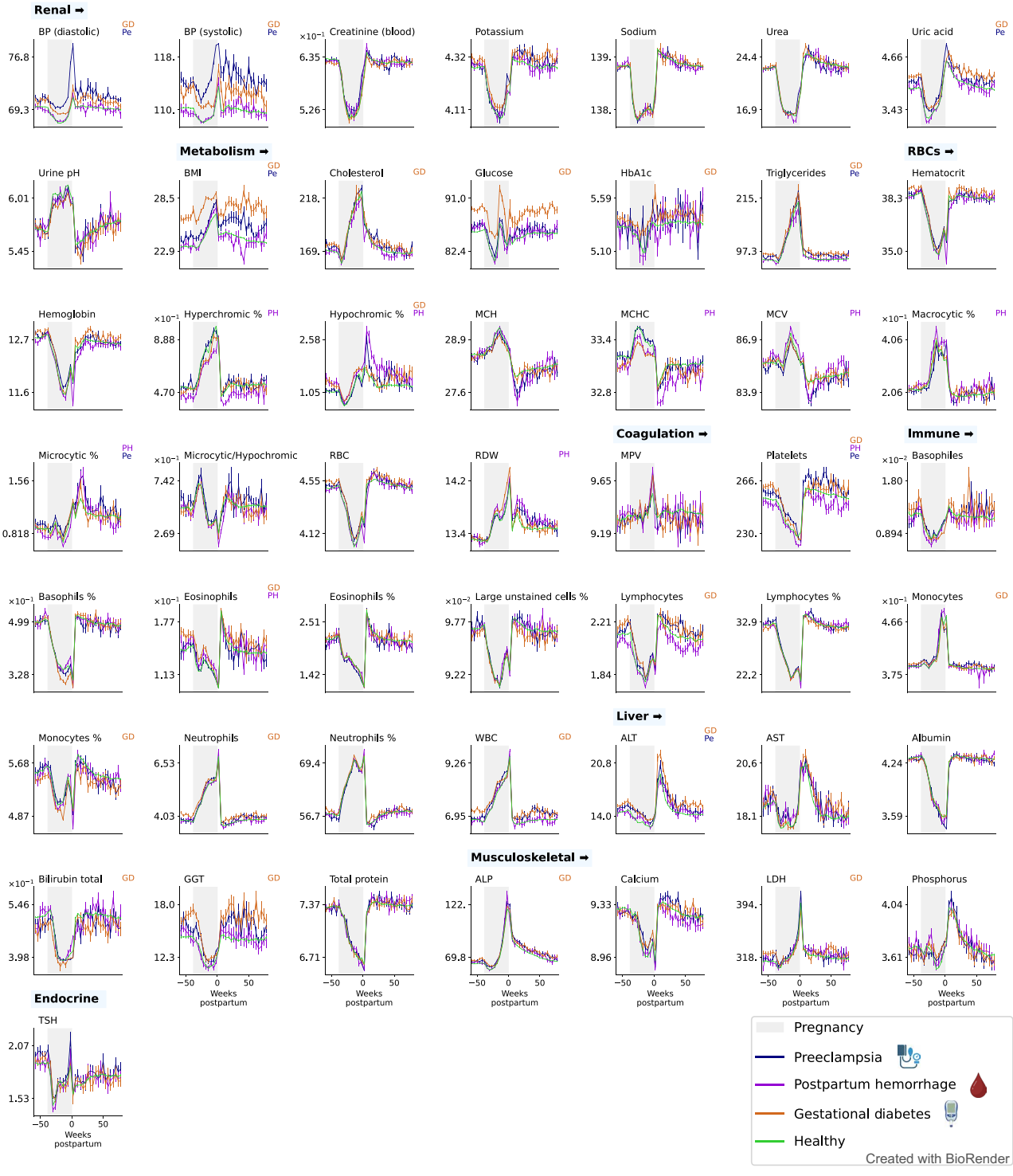

Fig. 5. Dynamics of lab tests in complications of pregnancy. Tests with significant differences from healthy pregnancy (green) are marked by Pe for preeclampsia (blue), PH for PPH (purple), and GD for gestational diabetes (orange). The *y* axis is different between tests; for units, see table S1. For the same figure with quantile scores, see fig. S5. Created with BioRender.

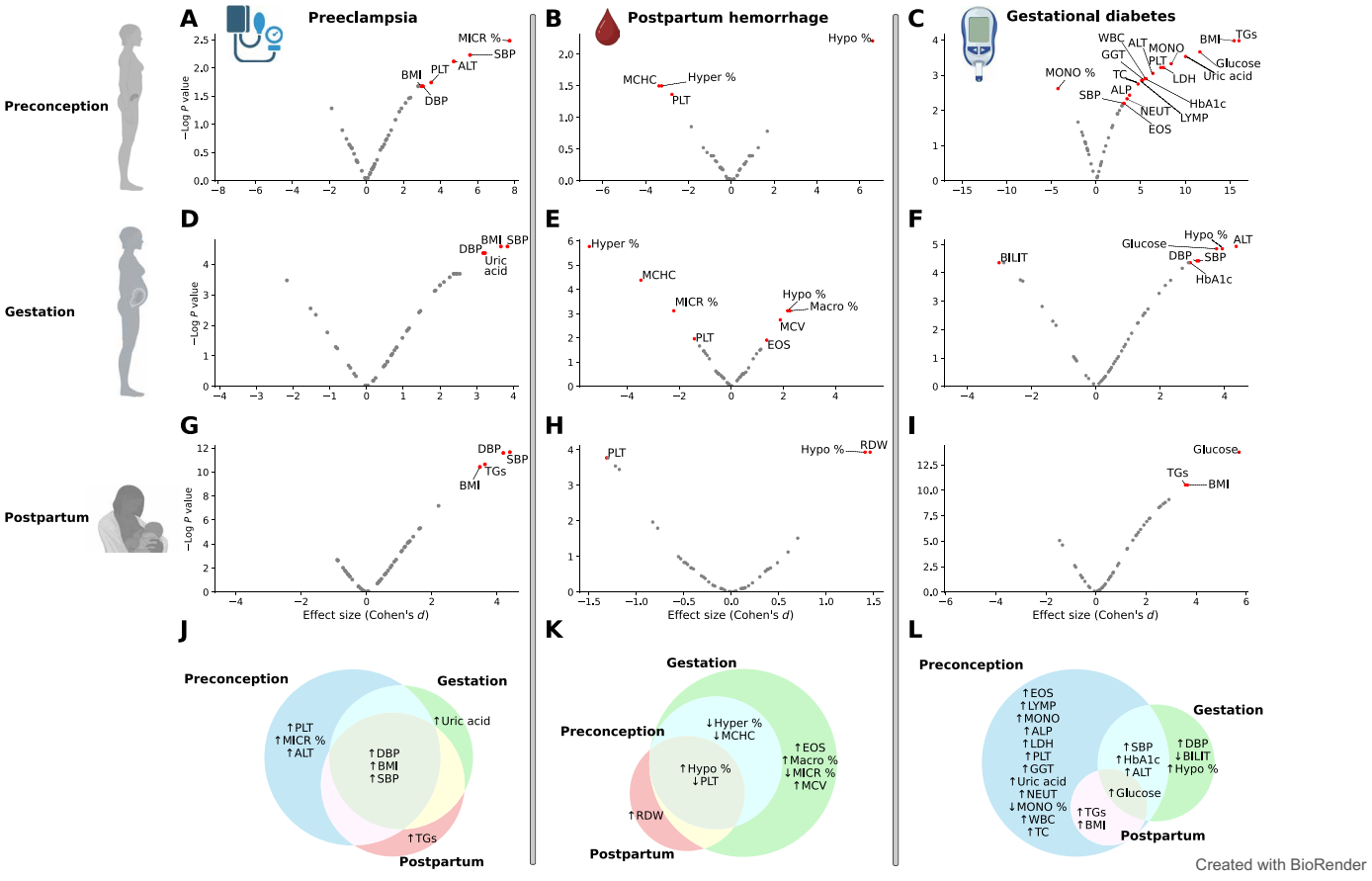

Fig. 6. Tests with significant deviations from healthy pregnancies in preeclampsia, gestational diabetes, and PPH. (**A** to **I**) Volcano plots of −log *P* value (FDR corrected) versus effect size for each test at each time point. See full test names in table S1. Significant tests are marked with a red dot and their name (Methods). (**J** to **L**) Venn diagrams showing the significant tests in the preconception (blue), gestation (green), and postpartum (red) periods for each complication. Created with BioRender.

unprecedented in terms of number of participants and time intervals and covers all major laboratory tests. About half of the tests take on the order of months to a year to return to baseline after delivery, highlighting the physiological aftermath of pregnancy. During gestation, all tests show sizable changes, and about half show large overshoots after delivery. The precision of the dataset allows detection of intricate dynamical changes, including the impact of preconception supplements and the deviations from healthy pregnancy in preeclampsia, gestational diabetes, and PPH. This study thus provides a resource for understanding pregnancy and the postpartum period and demonstrates how it may be used to understand mechanisms in systems physiology.

This study greatly expands our knowledge of the postpartum period because most postpartum studies considered only one or a few time points. Rather than a "fourth trimester" with rapid return to baseline, there is a slow recovery of between 10 and 50 weeks for 31/76 of the tests. Examples of such slowly adapting tests are ALP, albumin, AST, and ALT as well as sodium and uric acid.

We find that the postpartum return of the tests to baseline occurs by a trajectory that differs from the trajectory of change during pregnancy, a phenomenon called hysteresis. Postpartum adaptation is a distinct physiological process and not merely the reverse of pregnancy dynamics.

Several tests show a difference between their preconception values and their values 80 weeks postpartum. These postpartum differences include elevated levels of the inflammation marker CRP and reduced corpuscular hemoglobin (MCH) and iron. The differences could result from postpartum behavioral changes and/or from lasting physiological effects of pregnancy. Telling these factors apart is a major question for future research.

The lab tests show two types of stereotypical profiles, either a smooth rise-and-fall, where delivery redirects the direction of change back to baseline, or jump-like, where delivery causes a sharp overshoot or undershoot. Rebounds and sharp reversals have not been systematically characterized previously because studying them requires many temporal intervals, which were lacking in most previous studies.

These profile shapes can be rationalized based on general physiological principles. Overshoots are consistent with a compensatory mechanism that grows during pregnancy and remains high after delivery causing overcompensation. An example of such compensation occurs in the thyroid axis, where thyroid functional mass grows during pregnancy under the control of TSH and hCG (human chorionic gonadotropin), increasing the capacity to produce thyroid hormones. This extra mass takes months to recover postpartum given the slow turnover of thyroid cells, causing overshoot dynamics

in thyroid hormones. The ability of endocrine glands to change mass has important beneficial functions, such as dynamic compensation of variation in physiological parameters (*49*). Gland mass changes add a timescale of months to hormone dynamics and contribute to hormone seasonality (*50*), explain subclinical endocrine diseases (*17*), and cause extended dysregulation after chronic stress is relieved (*51*).

Pathologies of pregnancy showed distinct temporal profiles in specific tests. These differences from healthy pregnancies were more pronounced before conception and after delivery than during gestation for many of the tests. Several aberrations were shared between two pathologies—gestational diabetes and preeclampsia—suggesting the possibility of a pan-complication signature.

This study presents detailed cross-sectional temporal trajectories of pregnancy and postpartum physiology. These trajectories reveal prolonged recovery times and overshoot effects of many tests after delivery, preconception dynamics of many tests, and perturbed tests in pregnancy complications at unprecedented detail. It suggests processes that allow the mother's physiology to adapt to the multisystemic load of pregnancy and to navigate the abrupt effects of delivery. The power of this dataset stems from having delivery as a well-defined temporal signpost, $t = 0$. A similar approach might be useful for understanding other temporal transitions such as growth and development in childhood, puberty, menopause, and the course of specific diseases (diagnosed at $t = 0$) and their recovery processes. We hope that the present dataset will lead to a better understanding of pregnancy and postpartum biology and inspire similar studies of other crucial physiological processes that unfold over time.

Limitations of the study

This study has limitations associated with the use of medical datasets, including the effects of ascertainment bias. This study considered pregnancies in a single country; future work can consider effects of different locales. The study is cross-sectional and should be tested by future longitudinal studies that can assess subtypes of pregnancy trajectories. Thyroid tests are known to show low ergodicity (*52*, *53*), in the sense that an individual's test values vary over a small part of the population range. As a result, it is challenging to draw reliable conclusions about an individual's health by using population-wide reference values (*54*, *55*) because cross-sectional analysis could mask the changing trends of individuals.

METHODS

Study population

The study population consisted of individuals from the Clalit Healthcare database (*11*, *56*). We considered all pregnancies of females aged 20 to 35 between 2003 and 2020. For more information, see "stats.csv" and the "README.md" files in the GitHub repository.

Data collection

Medical records were pseudonymized by hashing of personal identifiers and randomization of dates by a random number of weeks uniformly sampled between 0 and 13 weeks for each patient and adding it to all dates in the patient diagnoses, laboratory, and medication records. This randomization does not affect timing relative to delivery. Retrospective test results were aggregated, and only statistical information was kept. Our ethical agreement with Clalit does not require informed consent for publication of this aggregated data.

We examined the time frame of 60 weeks before delivery to 80 weeks after delivery for all documented deliveries within our study population. We identified deliveries by ICD9 code V27 and confirmed a childbirth record for the individual. We excluded preterm deliveries (<37 weeks, ICD9 code 644), stillbirths, and deliveries with more than one newborn.

To mitigate ascertainment bias, for each test, we removed data from individuals with chronic disease that affects the test if the onset of the disease was up to 6 months after the test. We also removed data from individuals who purchased drugs, which affected the tests in the 6 months before the tests. Chronic diseases are defined as nonpediatric ICD9 codes with a Kaplan-Meier survival drop of >10% over 5 years. A list of chronic diseases can be found under "excluded_icd9_codes.csv" in the GitHub repository. Drugs that affect a test were defined as drugs with significant effect on the test [false discovery rate (FDR) < 0.01]. This step allowed us to focus on a relatively healthy subset of the pregnant population, reducing the confounding effects associated with the specific health conditions listed above or medication usage (*12*).

To exclude the potential effect of follow-up pregnancies in the 80 weeks following delivery, we excluded lab values from individuals with another delivery within 60 weeks following the measurement.

For each pregnancy, we gathered all available test values including standard blood count, kidney and liver function tests, blood coagulation tests, lipid panel, inflammation markers, and hormones (table S1). We then discretized test values into time points relative to the time of birth in weekly intervals for each test. In addition to test values, we also extracted data on patients including age (at measurement, mean, and interquartile range) and BMI (the most proximal BMI measurement in medical records before pregnancy, mean, and interquartile range, if available).

Quantile transformation

We transformed each measurement into a quantile score, normalized between 0 and 1. Quantiles were computed from cumulative distributions of test values from a reference population of age-matched nonpregnant females ($F_{test,age}$). The nonpregnant reference population included healthy nonmedicated females according to the R package LabNorm (*12*), including individuals in the study cohort during the time periods that they were not pregnant. The transformation is summarized as

$$\text{quantile\_score} = F_{test,age}(\text{value})$$

Data aggregation

Each individual test result included the age, latest BMI (if available), week postpartum (with 0 being delivery), and the quantile score. We aggregated the data into summary statistics: For each weekly interval per lab test, we calculated the mean, SD, and (5, 10, 25, 50, 75, 90, and 95)th percentiles of all the abovementioned data types. To obtain a test value at the mean quantile score for Figs. 1 and 5, we performed a back-transformation by transforming mean quantiles into test level values. The back-transformation uses a sparsely sampled cumulative distribution function per test (denoted F^{-1} below) and linear interpolation between the quantiles. The values for F^{-1} were queried using LabNorm and can be found in the attached git repo in a file named "Labnorm.csv." Tests without such a reference were filtered (see Data filtering below). Age parameterizing the back-transform is the median age of the population at the same week (week i below) as the mean quantile back-transformed

$$mean\_value_i = F^{-1}{}_{test,age_i}\left(mean\_quantile\_score_i\right)$$

Error bars are quantile SEM likewise back-transformed to test values (table S2). Fluctuations between neighboring points suggest additional errors on the order of 40 to 180% of SEM.

Data filtering
The original dataset included 110 tests. We excluded 31 tests with a small number of test results. If the SEM at any weekly interval, or the mean across all intervals, exceeded a threshold, the test was considered noisy. Three more tests were discarded with this procedure. For filtered tests and thresholds, see tables S2 and S3.

Data analysis
Unless otherwise stated, the mean quantile values were used for each test and weekly interval. See Quantile transformation and Data aggregation above for more details.

Averaging consecutive time points (smoothing)
In Fig. 1C, we smoothed the curves for tests with smaller sample sizes by using averaged consecutive weekly intervals. This process was performed for visualization and was not used for data analysis. See fig. S3 for the data without smoothing.

Dynamic range
We assessed the dynamic range across pregnancy by comparing the time intervals with the minimum and maximum values for each test. We performed a two-sample t test for each test between these time intervals with correction for FDR by the Benjamini-Hochberg method with a threshold of 0.05 using the "statsmodels" Python package.

Clustering
We performed clustering to group together tests with similar profiles. Tests were clustered (ward) using a distance metric of $1 - r_s$ where r_s is the Spearman correlation and "fcluster" from the python module "scipy.clustering.hierarchy." Each test is a vector of the quantile score at each of the 140-week intervals. For more information, see fig. S4.

Principal components analysis
We performed PCA using the python package "sklearn."

Settling time
We define the postpartum baseline using the quantile values in the last 10 weeks of the dataset, namely, weeks 70 to 80 after delivery, and define SDs using the average of the SDs of test values in these 10 bins. We next smoothed the mean test value data using a Gaussian kernel smoother, using the "gaussian_filter" function of the python "scipy.ndimage" module with sigma = 1 and mode = "nearest". The settling time is the time after which at least 90% of the smoothed time points remain within 0.2 SDs of the baseline values. The cutoff of 0.2 SDs was chosen by a visual inspection of the data. In Fig. 3, settling time was computed from quantile scores.

Preconception dynamics
We used linear regression to model the relationship between the test mean quantile score and time (in weeks) in the preconception period (60 to 38 weeks before delivery). We considered a test to have a notable dynamical trend if the absolute value of the regression line slope was greater than 0.1 and the P value was less than 0.05 after controlling for FDR. Linear regression was performed using "curve_fit" from python "scipy.optimize."

Data processing (pregnancy complications)
The methodology mentioned above was used to create a dataset of pregnancies with diagnosis of preeclampsia, gestational diabetes, and PPH using the ICD9 codes 642.4-9 excluding 642.8, (648.83 and 648.81) excluding 250 (diabetes), and 666, respectively. The measurement was included if the diagnosis was made not more than 140 weeks before/after the measurement was taken, and if the diagnosis was made in the [−42, +3] week where 0 denotes delivery. The test results were aggregated at a 4-week interval due to a lower number of measurements. Filtering as mentioned above yielded a subset of 50 tests, for a list, see table S1.

Data analysis (pregnancy complications)
Test results for each condition (preeclampsia, gestational diabetes, and PPH) were compared against the unaffected dataset aggregated at a 4-week interval. We performed a paired t test and separated the weekly intervals to preconception, gestation, and postpartum. We corrected for multiple comparisons using the Benjamini-Hochberg method with a threshold of <0.05, and Cohen's d as the effect size for a paired t test. We set effect size thresholds corresponding to large effect sizes (*57*, *58*) by visual inspection, as follows: preeclampsia ≥ 3.0, PPH ≥ 1.3, and gestational diabetes ≥ 3.0.

Supplementary Materials
This PDF file includes:
Supplementary Text
Figs. S1 to S5
Tables S1 to S3
References

REFERENCES AND NOTES

1. A. Mockridge, K. Maclennan, Physiology of pregnancy. *Anaesth. Intensive Care Med.* **20**, 397–401 (2019).
2. G. Mor, I. Cardenas, The immune system in pregnancy: A unique complexity. *Am. J. Reprod. Immunol.* **63**, 425–433 (2010).
3. P. Soma-Pillay, C. Nelson-Piercy, H. Tolppanen, A. Mebazaa, Physiological changes in pregnancy. *Cardiovasc. J. Afr.* **27**, 89–94 (2016).
4. V. L. Clifton, M. J. Stark, A. Osei-Kumah, N. A. Hodyl, The feto-placental unit, pregnancy pathology and impact on long term maternal health. *Placenta* **33**, S37–S41 (2012).
5. S. Chandra, A. K. Tripathi, S. Mishra, M. Amzarul, A. K. Vaish, Physiological changes in hematological parameters during pregnancy. *Indian J. Hematol. Blood Transfus.* **28**, 144–146 (2012).
6. S. Parrettini, A. Caroli, E. Torlone, Nutrition and metabolic adaptations in physiological and complicated pregnancy: Focus on obesity and gestational diabetes. *Front. Endocrinol.* **11**, 611929 (2020).
7. G. Chauhan, P. Tadi, "Physiology, postpartum changes" in *StatPearls* (StatPearls Publishing, 2022).
8. CDC, Pregnancy Complications, Maternal Infant Health (2024), https://cdc.gov/maternal-infant-health/pregnancy-complications/index.html.
9. M. Abbassi-Ghanavati, L. G. Greer, F. G. Cunningham, Pregnancy and laboratory studies: A reference table for clinicians. *Obstet. Gynecol.* **114**, 1326 (2009).
10. A. Larsson, M. Palm, L.-O. Hansson, O. Axelsson, Reference values for clinical chemistry tests during normal pregnancy. *BJOG* **115**, 874–881 (2008).
11. R. D. Balicer, A. Afek, Digital health nation: Israel's global big data innovation hub. *Lancet* **389**, 2451–2453 (2017).
12. N. M. Cohen, O. Schwartzman, R. Jaschek, A. Lifshitz, M. Hoichman, R. Balicer, L. I. Shlush, G. Barbash, A. Tanay, Personalized lab test models to quantify disease potentials in healthy individuals. *Nat. Med.* **27**, 1582–1591 (2021).
13. B. King, A. Spikesman, A. E. H. Emery, The effect of pregnancy on serum levels of creatine kinase. *Clin. Chim. Acta* **36**, 267–269 (1972).
14. M. E. Kotas, R. Medzhitov, Homeostasis, inflammation, and disease susceptibility. *Cell* **160**, 816–827 (2015).

15. S. Mangan, U. Alon, Structure and function of the feed-forward loop network motif. *Proc. Natl. Acad. Sci. U.S.A.* **100**, 11980–11985 (2003).
16. U. Alon, "The feedforward loop network motif" in *An Introduction to Systems Biology: Design Principles of Biological Circuits* (CRC Press, ed. 2, 2019), pp. 37–60.
17. Y. Korem Kohanim, T. Milo, M. Raz, O. Karin, A. Bar, A. Mayo, N. Mendelson Cohen, Y. Toledano, U. Alon, Dynamics of thyroid diseases and thyroid-axis gland masses. *Mol. Syst. Biol.* **18**, e10919 (2022).
18. A. D. Smethers, J. C. Trabulsi, V. A. Stallings, M. A. Papas, J. A. Mennella, Factors affecting BMI changes in mothers during the first year postpartum. *Nutrients* **15**, 1364 (2023).
19. C. S. Kovacs, "Calcium and phosphate metabolism and related disorders during pregnancy and lactation" in *Endotext*, K. R. Feingold, B. Anawalt, M. R. Blackman, A. Boyce, G. Chrousos, E. Corpas, W. W. de Herder, K. Dhatariya, K. Dungan, J. Hofland, S. Kalra, G. Kaltsas, N. Kapoor, C. Koch, P. Kopp, M. Korbonits, C. S. Kovacs, W. Kuohung, B. Laferrère, M. Levy, E. A. McGee, R. McLachlan, M. New, J. Purnell, R. Sahay, F. Singer, M. A. Sperling, C. A. Stratakis, D. L. Trence, D. P. Wilson, Eds. (MDText Inc., 2000).
20. D. R. Zimmerman, M. Kaplan, H. Shoob, M. Freisthler, M. Toledano, C. Stein-Zamir, Breastfeeding challenges and support in a high initiation population. *Isr. J. Health Policy Res.* **11**, 31 (2022).
21. Y. Amitai, N. Fisher, H. Meiraz, N. Baram, M. Tounis, A. Leventhal, Preconceptional folic acid utilization in Israel: Five years after the guidelines. *Prev. Med.* **46**, 166–169 (2008).
22. A. Reiss, M. J. Cohen, E. Kaliner, E. Gabai Kapara, A. Singer, I. Grotto, R. Gamzu, Lower rates of neural tube defects in Israel following folic acid supplementation policy. *Prev. Med.* **139**, 106064 (2020).
23. S. Azimi, E. Faramarzi, P. Sarbakhsh, A. Ostadrahimi, M. H. Somi, M. Ghayour, Folate and vitamin B12 status and their relation to hematological indices in healthy adults of Iranians: Azar cohort study. *Nutr. Health* **25**, 29–36 (2019).
24. A. de Azevedo Paiva, P. H. C. Rondó, E. M. Guerra-Shinohara, C. S. Silva, The influence of iron, vitamin B12, and folate levels on soluble transferrin receptor concentration in pregnant women. *Clin. Chim. Acta* **334**, 197–203 (2003).
25. P. S. Deol, T. A. Barnes, K. Dampier, K. J. Pasi, C. Oppenheimer, S. R. Pavord, The effects of folic acid supplements on coagulation status in pregnancy. *Br. J. Haematol.* **127**, 204–208 (2004).
26. O. Asbaghi, D. Ashtary-Larky, R. Bagheri, B. Nazarian, H. Pourmirzaei Olyaei, M. Rezaei Kelishadi, M. Nordvall, A. Wong, F. Dutheil, A. A. Naeini, Beneficial effects of folic acid supplementation on lipid markers in adults: A GRADE-assessed systematic review and dose-response meta-analysis of data from 21,787 participants in 34 randomized controlled trials. *Crit. Rev. Food Sci. Nutr.* **62**, 8435–8453 (2022).
27. O. Asbaghi, D. Ashtary-Larky, R. Bagheri, S. P. Moosavian, B. Nazarian, R. Afrisham, M. R. Kelishadi, A. Wong, F. Dutheil, K. Suzuki, A. Alavi Naeini, Effects of folic acid supplementation on inflammatory markers: A grade-assessed systematic review and dose–response meta-analysis of randomized controlled trials. *Nutrients* **13**, 2327 (2021).
28. M. Dott, S. A. Rasmussen, C. J. Hogue, J. Reefhuis, National Birth Defects Prevention Study, Association between pregnancy intention and reproductive-health related behaviors before and after pregnancy recognition, National Birth Defects Prevention Study, 1997–2002. *Matern. Child Health J.* **14**, 373–381 (2010).
29. B. T. Bateman, M. F. Berman, L. E. Riley, L. R. Leffert, The epidemiology of postpartum hemorrhage in a large, nationwide sample of deliveries. *Anesth. Analg.* **110**, 1368 (2010).
30. T. Sella, V. Shalev, U. Elchalal, A. Chovel-Sella, G. Chodick, Screening for gestational diabetes in the 21st century: A population-based cohort study in Israel. *J. Matern. Fetal Neonatal Med.* **26**, 412–416 (2013).
31. D. S. Seidman, P. Ever-Hadani, D. K. Stevenson, R. Gale, The effect of abortion on the incidence of pre-eclampsia. *Eur. J. Obstet. Gynecol. Reprod. Biol.* **33**, 109–114 (1989).
32. E. Dimitriadis, D. L. Rolnik, W. Zhou, G. Estrada-Gutierrez, K. Koga, R. P. V. Francisco, C. Whitehead, J. Hyett, F. da Silva Costa, K. Nicolaides, E. Menkhorst, Pre-eclampsia. *Nat. Rev. Dis. Primers.* **9**, 8 (2023).
33. M. S. Kramer, M. Dahhou, D. Vallerand, R. Liston, K. S. Joseph, Risk factors for postpartum hemorrhage: Can we explain the recent temporal increase? *J. Obstet. Gynaecol. Can.* **33**, 810–819 (2011).
34. L. K. Wagner, Diagnosis and management of preeclampsia. *Am. Fam. Physician* **70**, 2317–2324 (2004).
35. D. Altman, G. Carroli, L. Duley, B. Farrell, J. Moodley, J. Neilson, D. Smith, Magpie Trial Collaboration Group, Do women with pre-eclampsia, and their babies, benefit from magnesium sulphate? The Magpie Trial: A randomised placebo-controlled trial. *Lancet* **359**, 1877–1890 (2002).
36. J. M. Roberts, P. A. August, G. Bakris, J. R. Barton, I. M. Bernstein, M. Druzin, R. R. Gaiser, J. P. Granger, A. Jeyabalan, D. D. Johnson, S. A. Karumanchi, M. Lindheimer, M. Y. Owens, G. R. Saade, B. M. Sibai, C. Y. Spong, E. Tsigas, G. E. Joseph, N. O'Reilly, A. Politzer, S. Son, K. Ngaiza, Hypertension in pregnancy: Executive summary. *Obstet. Gynecol.* **122**, 1122 (2013).
37. E. A. Phipps, R. Thadhani, T. Benzing, S. A. Karumanchi, Pre-eclampsia: Pathogenesis, novel diagnostics and therapies. *Nat. Rev. Nephrol.* **15**, 275–289 (2019).
38. K. C. Wormer, R. T. Jamil, S. B. Bryant, "Acute postpartum hemorrhage" in *StatPearls* (StatPearls Publishing, 2024).
39. J. L. Bienstock, A. C. Eke, N. A. Hueppchen, Postpartum hemorrhage. *N. Engl. J. Med.* **384**, 1635–1645 (2021).
40. Committee on Practice Bulletins-Obstetrics, Practice bulletin no. 183: Postpartum hemorrhage. *Obstet. Gynecol.* **130**, e168–e186 (2017).
41. A. Gillissen, T. van den Akker, C. Caram-Deelder, D. D. C. A. Henriquez, K. W. M. Bloemenkamp, M. P. M. de Maat, J. J. M. van Roosmalen, J. J. Zwart, J. Eikenboom, J. G. van der Bom, TeMpOH-1 Study Group, Coagulation parameters during the course of severe postpartum hemorrhage: A nationwide retrospective cohort study. *Blood Adv.* **2**, 2433–2442 (2018).
42. S. C. Reale, S. R. Easter, X. Xu, B. T. Bateman, M. K. Farber, Trends in postpartum hemorrhage in the United States from 2010 to 2014. *Anesth. Analg.* **130**, e119 (2020).
43. M. R. Robinson, M. Patxot, M. Stojanov, S. Blum, D. Baud, Postpartum hemorrhage risk is driven by changes in blood composition through pregnancy. *Sci. Rep.* **11**, 19238 (2021).
44. H. D. McIntyre, P. Catalano, C. Zhang, G. Desoye, E. R. Mathiesen, P. Damm, Gestational diabetes mellitus. *Nat. Rev. Dis. Primer.* **5**, 47 (2019).
45. W. Ye, C. Luo, J. Huang, C. Li, Z. Liu, F. Liu, Gestational diabetes mellitus and adverse pregnancy outcomes: Systematic review and meta-analysis. *BMJ* **377**, e067946 (2022).
46. G. T. Prakash, A. K. Das, S. Habeebullah, V. Bhat, S. B. Shamanna, Maternal and neonatal outcome in mothers with gestational diabetes mellitus. *Indian J. Endocrinol. Metab.* **21**, 854–858 (2017).
47. G. Chodick, U. Elchalal, T. Sella, A. D. Heymann, A. Porath, E. Kokia, V. Shalev, The risk of overt diabetes mellitus among women with gestational diabetes: A population-based study. *Diabet. Med.* **27**, 779–785 (2010).
48. R. Fox, J. Kitt, P. Leeson, C. Y. L. Aye, A. J. Lewandowski, Preeclampsia: Risk factors, diagnosis, management, and the cardiovascular impact on the offspring. *J. Clin. Med.* **8**, 1625 (2019).
49. O. Karin, A. Swisa, B. Glaser, Y. Dor, U. Alon, Dynamical compensation in physiological circuits. *Mol. Syst. Biol.* **12**, 886 (2016).
50. A. Tendler, A. Bar, N. Mendelsohn-Cohen, O. Karin, Y. Korem Kohanim, L. Maimon, T. Milo, M. Raz, A. Mayo, A. Tanay, U. Alon, Hormone seasonality in medical records suggests circannual endocrine circuits. *Proc. Natl. Acad. Sci. U.S.A.* **118**, e2003926118 (2021).
51. O. Karin, M. Raz, A. Tendler, A. Bar, Y. Korem Kohanim, T. Milo, U. Alon, A new model for the HPA axis explains dysregulation of stress hormones on the timescale of weeks. *Mol. Syst. Biol.* **16**, e9510 (2020).
52. R. Hoermann, J. E. M. Midgley, R. Larisch, J. W. Dietrich, Individualised requirements for optimum treatment of hypothyroidism: Complex needs, limited options. *Drugs Context* **8**, 212597 (2019).
53. S. Andersen, K. M. Pedersen, N. H. Bruun, P. Laurberg, Narrow individual variations in serum T4 and T3 in normal subjects: A clue to the understanding of subclinical thyroid disease. *J. Clin. Endocrinol. Metab.* **87**, 1068–1072 (2002).
54. A. J. Fisher, J. D. Medaglia, B. F. Jeronimus, Lack of group-to-individual generalizability is a threat to human subjects research. *Proc. Natl. Acad. Sci. U.S.A.* **115**, E6106–E6115 (2018).
55. R. Hoermann, J. E. M. Midgley, R. Larisch, J. W. Dietrich, Functional and symptomatic individuality in the response to levothyroxine treatment. *Front. Endocrinol.* **10**, 664 (2019).
56. N. M. Cohen, A. Lifshitz, R. Jaschek, E. Rinott, R. Balicer, L. I. Shlush, G. I. Barbash, A. Tanay, Longitudinal machine learning uncouples healthy aging factors from chronic disease risks. *Nat. Aging* **4**, 129–144 (2024).
57. D. Lakens, Calculating and reporting effect sizes to facilitate cumulative science: A practical primer for t-tests and ANOVAs. *Front. Psychol.* **4**, 863 (2013).
58. J. Cohen, "The t test for means" in *Statistical Power Analysis for the Behavioral Sciences* (Routledge, ed. 2, 1988), pp. 19–74.
59. K. L. Cheung, R. A. Lafayette, Renal physiology of pregnancy. *Adv. Chronic Kidney Dis.* **20**, 209–214 (2013).
60. A. Odutayo, M. Hladunewich, Obstetric nephrology: Renal hemodynamic and metabolic physiology in normal pregnancy. *Clin. J. Am. Soc. Nephrol.* **7**, 2073 (2012).
61. R. R. Bailey, G. L. Rolleston, Kidney length and ureteric dilatation in the puerperium. *J. Obstet. Gynaecol. Br. Commonw.* **78**, 55–61 (1971).
62. S. Gowda, P. B. Desai, S. S. Kulkarni, V. V. Hull, A. A. K. Math, S. N. Vernekar, Markers of renal function tests. *N. Am. J. Med. Sci.* **2**, 170–173 (2010).
63. O. Ogueh, A. Clough, M. Hancock, M. R. Johnson, A longitudinal study of the control of renal and uterine hemodynamic changes of pregnancy. *Hypertens. Pregnancy* **30**, 243–259 (2011).
64. T. Lind, K. A. Godfrey, H. Otun, P. R. Philips, Changes in serum uric acid concentrations during normal pregnancy. *BJOG* **91**, 128–132 (1984).
65. L. M. Dalton, D. M. Ní Fhloinn, G. T. Gaydadzhieva, O. M. Mazurkiewicz, H. Leeson, C. P. Wright, Magnesium in pregnancy. *Nutr. Rev.* **74**, 549–557 (2016).
66. J. P. De Flamingh, J. V. van der Merwe, A serum biochemical profile of normal pregnancy. *S. Afr. Med. J.* **65**, 552–555 (1984).
67. R. Sefa, E. H. Cetin, K. Gurkan, K. Metin, Are changes in urinary parameters during pregnancy clinically significant? *Urol. Res.* **34**, 244–248 (2006).

68. G. Lee, S. Kim, H. Park, J. Lee, J. P. Lee, Y. Kho, G. Choi, J. Park, S. Worakhunpiset, H.-B. Moon, K. Choi, Variability of urinary creatinine, specific gravity, and osmolality over the course of pregnancy: Implications in exposure assessment among pregnant women. *Environ. Res.* **198**, 110473 (2021).
69. Y. Bacq, *The Liver in Normal Pregnancy* (Landes Bioscience, 2013).
70. J. T. Busher, "Serum albumin and globulin" in *Clinical Methods: The History, Physical, and Laboratory Examinations*, H. K. Walker, W. D. Hall, J. W. Hurst, Eds. (Butterworths, ed. 3, 1990).
71. Y. Bacq, O. Zarka, J. F. Bréchot, N. Mariotte, S. Vol, J. Tichet, J. Weill, Liver function tests in normal pregnancy: A prospective study of 103 pregnant women and 103 matched controls. *Hepatology* **23**, 1030–1034 (1996).
72. N. N. Than, J. Neuberger, Liver abnormalities in pregnancy. *Best Pract. Res. Clin. Gastroenterol.* **27**, 565–575 (2013).
73. G. Chemnitz, L. Nevermann, E. Schmidt, F. W. Schmidt, J. Lobers, Creatine kinase (EC-No.2.7.3.2) and creatine kinase isoenzymes during pregnancy and labor and in the cord blood. *Clin. Biochem.* **12**, 277–281 (1979).
74. C. S. Kovacs, Maternal mineral and bone metabolism during pregnancy, lactation, and post-weaning recovery. *Physiol. Rev.* **96**, 449–547 (2016).
75. M. Sanghavi, J. D. Rutherford, Cardiovascular physiology of pregnancy. *Circulation* **130**, 1003–1008 (2014).
76. J. M. Higgins, Red blood cell population dynamics. *Clin. Lab. Med.* **35**, 43–57 (2015).
77. J. D. Bessman, P. R. Gilmer, F. H. Gardner, Improved classification of anemias by MCV and RDW. *Am. J. Clin. Pathol.* **80**, 322–326 (1983).
78. J. W. Choi, M. W. Im, S. H. Pai, Serum transferrin receptor concentrations during normal pregnancy. *Clin. Chem.* **46**, 725–727 (2000).
79. A. L. Fisher, E. Nemeth, Iron homeostasis during pregnancy. *Am. J. Clin. Nutr.* **106**, 1567S–1574S (2017).
80. B. Abu-Raya, C. Michalski, M. Sadarangani, P. M. Lavoie, Maternal immunological adaptation during normal pregnancy. *Front. Immunol.* **11**, 575197 (2020).
81. C. Paccolat, S. Harbarth, D. Courvoisier, O. Irion, B. M. de Tejada, Procalcitonin levels during pregnancy, delivery and postpartum. *J. Perinat. Med.* **39**, 679–683 (2011).
82. B. Brenner, Haemostatic changes in pregnancy. *Thromb. Res.* **114**, 409–414 (2004).
83. J. Dai, P. Mao, C. Pu, X. Wang, X. Liu, Trimester-specific reference intervals and profile of coagulation parameters for Chinese pregnant women with diverse demographics and obstetric history: A cross-sectional study. *BMC Pregnancy Childbirth* **23**, 421 (2023).
84. A. M. Ciobanu, S. Colibaba, B. Cimpoca, G. Peltecu, A. M. Panaitescu, Thrombocytopenia in pregnancy. *Maedica* **11**, 55–60 (2016).
85. Z. N. Pascual, M. D. Langaker, "Physiology, pregnancy" in *StatPearls* (StatPearls Publishing, 2024).
86. P. M. Catalano, E. D. Tyzbir, N. M. Roman, S. B. Amini, E. A. Sims, Longitudinal changes in insulin release and insulin resistance in nonobese pregnant women. *Am. J. Obstet. Gynecol.* **165**, 1667–1672 (1991).
87. S. N. Hinkle, M. Y. Tsai, S. Rawal, P. S. Albert, C. Zhang, HbA_{1c} measured in the first trimester of pregnancy and the association with gestational diabetes. *Sci. Rep.* **8**, 12249 (2018).
88. U. Kampmann, S. Knorr, J. Fuglsang, P. Ovesen, Determinants of maternal insulin resistance during pregnancy: An updated overview. *J. Diabetes Res.* **2019**, 5320156 (2019).
89. D. F. M. Loke, O. A. C. Viegas, L. P. Kek, M. Rauff, A. C. Thai, S. S. Ratnam, Lipid profiles during and after normal pregnancy. *Gynecol. Obstet. Invest.* **32**, 144–147 (2010).
90. R. H. Knopp, C. E. Walden, P. W. Wahl, R. Bergelin, M. Chapman, S. Irvine, J. J. Albers, Effect of postpartum lactation on lipoprotein lipids and apoproteins. *J. Clin. Endocrinol. Metab.* **60**, 542–547 (1985).
91. C. Muñoz-Manrique, B. Trejo-Valdivia, S. Hernández-Cordero, A. Cantoral, A. L. Deierlein, E. Colicino, M. M. Niedzwiecki, R. O. Wright, A. A. Baccarelli, M. M. Téllez-Rojo, Weight gain trajectories patterns from pregnancy to early postpartum: Identifying women at risk and timing to prevent weight regain. *BMC Pregnancy Childbirth* **22**, 811 (2022).
92. D. Springer, J. Jiskra, Z. Limanova, T. Zima, E. Potlukova, Thyroid in pregnancy: From physiology to screening. *Crit. Rev. Clin. Lab. Sci.* **54**, 102–116 (2017).
93. T. I. M. Korevaar, M. Medici, T. J. Visser, R. P. Peeters, Thyroid disease in pregnancy: New insights in diagnosis and clinical management. *Nat. Rev. Endocrinol.* **13**, 610–622 (2017).
94. P. Cignini, E. V. Cafà, C. Giorlandino, S. Capriglione, A. Spata, N. Dugo, Thyroid physiology and common diseases in pregnancy: Review of literature. *J. Prenat. Med.* **6**, 64–71 (2012).
95. A. Chatzitomaris, R. Hoermann, J. E. Midgley, S. Hering, A. Urban, B. Dietrich, A. Abood, H. H. Klein, J. W. Dietrich, Thyroid allostasis–adaptive responses of thyrotropic feedback control to conditions of strain, stress, and developmental programming. *Front. Endocrinol.* **8**, 163 (2017).
96. S. Y. Chan, E. Vasilopoulou, M. D. Kilby, The role of the placenta in thyroid hormone delivery to the fetus. *Nat. Clin. Pract. Endocrinol. Metab.* **5**, 45–54 (2009).
97. G. N. Burrow, D. A. Fisher, P. R. Larsen, Maternal and fetal thyroid function. *N. Engl. J. Med.* **331**, 1072–1078 (1994).
98. M. Yoshimura, J. M. Hershman, Thyrotropic action of human chorionic gonadotropin. *Thyroid* **5**, 425–434 (1995).
99. P. Laurberg, S. L. Andersen, P. Hindersson, E. A. Nohr, J. Olsen, Dynamics and predictors of serum TSH and fT4 reference limits in early pregnancy: A study within the Danish National Birth Cohort. *J. Clin. Endocrinol. Metab.* **101**, 2484–2492 (2016).
100. C. Li, Z. Shan, J. Mao, W. Wang, X. Xie, W. Zhou, C. Li, B. Xu, L. Bi, T. Meng, J. Du, S. Zhang, Z. Gao, X. Zhang, L. Yang, C. Fan, W. Teng, Assessment of thyroid function during first-trimester pregnancy: What is the rational upper limit of serum TSH during the first trimester in Chinese pregnant women? *J. Clin. Endocrinol. Metab.* **99**, 73–79 (2014).
101. R. Stricker, M. Echenard, R. Eberhart, M.-C. Chevailler, V. Perez, F. A. Quinn, R. Stricker, Evaluation of maternal thyroid function during pregnancy: The importance of using gestational age-specific reference intervals. *Eur. J. Endocrinol.* **157**, 509–514 (2007).
102. W. E. Visser, R. P. Peeters, Interpretation of thyroid function tests during pregnancy. *Best Pract. Res. Clin. Endocrinol. Metab.* **34**, 101431 (2020).

Acknowledgments: We thank all members of our lab and I. Solt, A. Tanay, and E. Segal for discussions. We thank G. Barabash and R. Balicer for the Clalit-Weizmann collaboration. Data acquisition was approved by the Clalit Helsinki Committee RMC-1059-20. **Funding:** This work was supported by the European Research Council (ERC) under the European Union's Horizon 2020 research and innovation program (grant agreement no. 856487). Y.K.K. is supported by the JSMF Postdoctoral Fellowship in Understanding Dynamic and Multi-scale Systems (https://doi.org/10.37717/2020-1428). **Author contributions:** Conceptualization: A.B., Y.K.K., Y.T., U.A., and R.M. Methodology: A.B., N.M.-C., A.M., R.M., Y.K.K., and U.A. Formal analysis: A.B., R.M., A.M., N.M.-C., and U.A. Funding acquisition: U.A. Visualization: A.B., R.M., and U.A. Data curation: N.M.-C., A.B., and Y.T. Supervision: U.A. Software: A.B. and R.M. Writing—original draft: A.B. and U.A. Writing—review and editing: R.M., A.B., U.A., and Y.T. **Competing interests:** The authors declare that they have no competing interests. **Data and materials availability:** All data needed to evaluate the conclusions in the paper are present in the paper and/or the Supplementary Materials. The source code and data used to perform the analysis are available at the GitHub repository as of the date of publication. The repository is open for public use: https://github.com/AlonLabWIS/PregnancyMillions. The full dataset is published on Dryad: https://doi.org/10.5061/dryad.1c59zw44t. A frozen code repository is available on Zenodo: https://doi.org/10.5281/zenodo.13996864.

Submitted 16 July 2024
Accepted 24 February 2025
Published 26 March 2025
10.1126/sciadv.adr7922